

# SoC Profile Reconstruction in Residential EV Charging: Assessing the Degradation of V1G and V2G in Denmark

M. Etxandi-Santolaya<sup>1,3</sup>, M. Secchi<sup>2</sup>, M. Marinelli<sup>2</sup>, L. Canals Casals<sup>3</sup>, C. Corchero<sup>4</sup> and J. Eichman<sup>1</sup>

<sup>1</sup> Department of Energy Systems Analytics  
Institut de Recerca en Energia de Catalunya—IREC  
08930 Sant Adrià de Besòs (Spain)

<sup>3</sup> Department of Engineering Projects and Construction  
Universitat Politècnica de Catalunya—UPC  
08034 Barcelona (Spain)

<sup>2</sup> Department of Wind and Energy Systems  
Danmarks Tekniske Universitet – DTU  
2800 Kgs. Lyngby (Denmark)

<sup>4</sup> Bamboo Energy,  
08018 Barcelona (Spain)

## Abstract.

The development of Smart Charging (SC) strategies for Electric Vehicles (EVs) is on the rise, driven by the potential benefits for both customers and grid operators. While several studies have explored the impact of these strategies on battery degradation, there is a lack of studies based on real-world data. To overcome the limited information provided by the current EV-EVSE (EV Supply Equipment) communication protocols, a methodology to reconstruct State of Charge (SoC) profiles based on the charging power is proposed and used to reconstruct the profiles and analyse the battery degradation for three residential EVSEs in Denmark, comparing degradation trends in under Uncontrolled Charging (UC) mode, with the SC ones. Results show that the economic profits from unidirectional (V1G) SC strategies based on price, offer significant cost savings (10-22% annually) and reduce calendar ageing by up to 4% over a decade. V2G strategies entail modest increases in cost savings at the cost of a minimal additional degradation.

**Keywords.** Battery Degradation, Electric Vehicle, Smart Charging, Vehicle to Grid

## 1. Introduction

The Electric Vehicle (EV) market is experiencing unprecedented growth, driven by environmental concerns, government incentives, and advancements in battery technology. As the number of EVs on the roads continues to increase, there is a growing focus on exploring innovative Smart Charging (SC) solutions including (V1G) SC and Vehicle-to-Grid (V2G) SC. V1G involves the up or down-modulation, or the shifting in time of the charging power profile in response to an external signal, which provides economic benefit for consumers and, eventually, enhances grid stability [1]. V2G services take the concept further by allowing EV batteries to also feed excess energy back into the grid, providing grid operators with additional

flexibility to manage fluctuations in both demand and supply [2].

Quantifying the impact of SC on the battery degradation is an important part of analysing their feasibility. The most critical SC is V2G, as the Ah throughput compared to Uncontrolled Charging (UC) mode is increased and thus the cycling ageing of the battery is higher. Indeed, in some studies, V2G was found to create a significant degradation, forcing an early battery retirement (e.g. up to 0.06% capacity fade daily [3] or twice the amount of weekly degradation compared to the baseline [4]). Some studies pointed out that this lifetime reduction can be as high as 35% for highly impactful grid services [5]. However other studies suggest that the impact of degradation is low, e.g. 0.38-1.18% fade after 10 years [6]. Some studies even argue that the reduced calendar ageing produced by shifting the charging session start to a later time and reducing its power, can compensate the increase in cycling, leading to a reduced overall degradation [7], [8], [9]. The results strongly depend on the assumptions, including the EV model and the driving behaviour. This latter is generally obtained from driving surveys in the form of daily mileages and schedules. Depending on the study, the driving trip is assumed to be constant [3], [4], [7], to follow a normal distribution [10] or obtained from a random sample from surveys [6], [11]. The SoC is generally obtained assuming a specific energy consumption and full charges.

None of the reviewed studies employs real-world charging profiles, assuming relatively uniform behaviours instead. When considering the use of real data an important challenge arises. Current communication standards (IEC 61851) do not support essential information exchange required for SC, with OCPP 2.0.1 and ISO15118-20 still being mostly not implemented [12], [13]. Consequently, critical variables like the nominal battery capacity or the SoC are not available.

This study addresses this lack of information by introducing a methodology to reconstruct SoC profiles, based on real-world data collected from residential EV chargers in Denmark. With the reconstructed profiles it is possible to evaluate battery degradation both from the UC behaviour and from the optimized SC profiles.

## 2. Data description and selection of locations

The dataset employed in this study comprises charging profiles from September 2021 to March 2023 measured at residential EV chargers installed throughout Denmark, and provided by Spirii, a local charging point operator. The dataset contains the timeseries of the AC power and the EV states (charging/idling/disconnected). This study focuses on a subset of the available locations, specifically targeting those that meet the following criteria:

- 1) The data must contain one full year.
- 2) The power profile must show a low correlation with the price. This allows filtering out EV owners who are already employing some form of SC.
- 3) More than 90% of the charging sessions must be considered complete.
- 4) No more than one consecutive incomplete charging session must be observed.

Note that criteria 3 and 4 are imposed by the SoC reconstruction methodology.

The selected chargers (C1, C2 and C3) show different charging power levels and usage characteristics, as presented in Table 1. Boxplots of energy charged per session are presented in Figure 1.

- C1 shows low energy charged per session and high frequency. This charger most-likely belongs to a Plug-in Hybrid EV (PHEV).
- C2 shows slightly higher energy charged per session compared to C1, which suggest that it could belong to a PHEV or a short-range BEV (Battery EV).
- C3 represents a user with a long-range BEV.

## 3. Methodology

The aim of this study is to compare, for the three selected locations, the degradation trends for the following charging strategies:

- **Uncontrolled Charging (UC):** represents the baseline behaviour of the users captured by the dataset.
- **Unidirectional SC (V1G):** represents the simplest form of SC not allowing the battery to be discharged.
- **Bidirectional SC (V2G):** the battery is allowed to discharge to the power system as well.

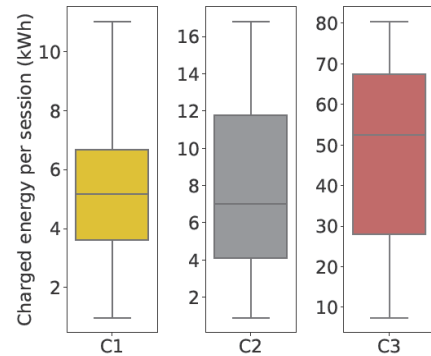


Figure 1. Energy per session for each charger.

### A. Capacity estimation

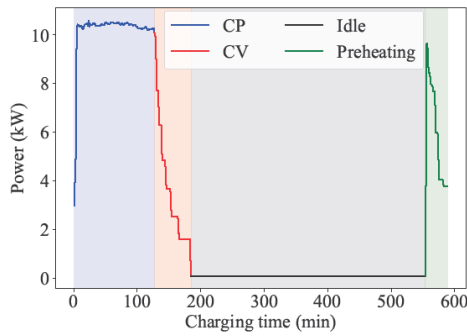
The nominal capacity in this study is estimated by multiplying the median of energy charged per session by a factor of 2 (corresponding to an average use of 50% of the battery [14]). In addition, the capacity is selected to guarantee that users will always reach the destination even at 80% SoH. Considering available models in the market, capacities over 95 kWh are not considered. Based on this, the estimated usable nominal capacities are 14, 21 and 95 kWh for C1, C2 and C3, respectively. Thus, C1 represents a PHEV and C2 and C3 a battery EV. Note how these values are “effective” battery capacities, so they consider a 0-100% SoC range, which is assumed to be 20% lower than the full capacity, as explained in Section 3D.

Table 1. Main characteristics of the selected charging locations.

	C1	C2	C3
Period	Mar22-Mar23	Sept21-Sept22	Oct21-Oct22
Number of sessions	233	113	44
Usable battery capacity (kWh)	14	21	95
Total energy consumed (MWh)	1.32	0.99	2.35
Median of energy charged per session (kWh)	5.64	7.21	56.85
Maximum energy charged in a session (kWh)	11.01	18.81	89.27
Median charging power during CP phase (kW)	3.55	6.91	10.98
Number of complete sessions (% of total)	98.7%	95.2%	97.7%
Median charging session duration (h)	15.5	7.8	12.9
Median SOC at connection	10 %	64%	46%
Idle time (plugged without charging over total)	37.10%	8.45%	3.83%
Connection time (plugged either charging or idling)	45.77%	10.27%	6.47 %

## B. SoC profile reconstruction

For the SoC reconstruction, the power profiles during the charging sessions are analysed. Firstly, the complete sessions are identified. This task is performed by assessing if the charging power gradually decays at the end, corresponding to the Constant Voltage (CV) phase of the session. This behaviour stems from modern battery management systems, limiting the charging voltage of the battery since charging at high SoC values requires overcoming a very high open circuit voltage. The first part of Figure 2 shows an example of a Constant Power (CP) phase followed by a CV phase. Conversely, incomplete sessions only show the CP phase and not the CV one. If less than 2 h are recorded between the end of an incomplete session and the beginning of the next one, it is assumed that they form a single session. Additionally, at the end of some sessions, during cold months, a distinct power profile is observed which most likely represents the preheating of the battery before driving (marked in green in Figure 2), and is thus excluded from the SC optimisation.



**Figure 2.** Example power profile during a charging session.

Once the charging sessions are classified as complete, incomplete, or complete with preheating, the SoC profile reconstruction is performed, according to the following steps.

1. First, the SoC for complete sessions is obtained considering that the charge ends at 100% and applying Coulomb Counting, which consists of integrating the current flowing into or out of the battery over time.
2. For the complete sessions with preheating, the point where the battery is fully charged is obtained and the SoC is assumed to be constant from that point until the end of the session, as the preheating is performed by drawing energy from the station. The SoC corresponding to the CP-CV charge is obtained as in the previous step.
3. For the incomplete sessions, the initial or final SoC is unknown. Consequently, the assumption is made that the driving trip preceding the charging session adheres to the user's typical behaviour, with an energy consumption  $T$  equivalent to the median of all documented trips. To minimize the impact of this assumption, criteria 3 was set in Section 2. The value of  $T$  is iteratively modified until it meets the following constraints:
  - The initial SoC of the  $n$ -th charging session, which is defined considering the trip consumption, must be positive.

- The final SoC needs to be below 90%. This upper limit is set considering that the charge is incomplete.
  - The final SoC needs to be higher than the initial SoC of the next session.
4. The previous steps allow to obtain the SoC during charging. During driving the SoC is obtained by linearization between the end of a charge and the start of the next one. Following this assumption, the power during driving is assumed to be constant.
  5. Whenever the battery is idling the SoC is constant.

Additionally, the daily mean temperature data are extracted from the Danish Meteorological Institute (DMI) website [15] based on the location and time. The power, SoC, and battery capacity, are the required inputs for the SC optimization algorithm.

## C. SC optimization algorithm

The EV SC scheduling was formulated as a mixed-integer linear programming (MILP) problem, with the aim of minimising the total charging costs for the EV owners. The objective function can be written as in Eq. 1:

$$\min_{\substack{P_{ch}; P_{dch} \\ Y_{ch}; Y_{dch}}} [c_{ch}^T \cdot P_{ch} + c_{dch}^T \cdot P_{dch}] \cdot \Delta t \quad (1)$$

where:

- $P_{ch}$  and  $P_{dch}$  are the decision variables column vectors containing the AC power absorbed by or extracted from each EV battery at each of the charging session instants.
- $Y_{ch}$  and  $Y_{dh}$  contain the binary variables which determine if the charging/discharging processes are ON (1) or OFF (0). They are not part of the objective function, but rather used in the constraints to limit the values of  $P_{ch}$  and  $P_{dch}$ .
- $c_{ch}$  and  $c_{dch}$  are the column vectors containing the EV charging costs (retail prices, including network tariffs and VAT) and the discharging compensation values (day-ahead market prices).
- $\Delta t$  is the simulation timestep in hours (10 min = 1/6 h).

Several constraints are imposed to ensure that the EV owner experience is not impacted by the smart charging strategies:

- **Min./Max. SoC:** for the optimisation, the full 0-100% capacity is used, but in general 10% min. SoC is considered in case of unforeseen circumstances, while a 90% max. SoC is considered to avoid excessive battery wear [16]. The 10-90% range is used for the degradation model, which runs on the full battery capacity instead of the usable one.
- **Min./Max. charging and discharging power levels:** the min. current is 6 A 1-ph (1.38 kW) [17], while the max. power is the highest power measured for each charger in the analysed period.
- **EV Battery Inverter Efficiency:** set to 90% (81% round-trip) [18], to account for losses in AC/DC conversion.

- **Energy at disconnection:** the energy charged in the EV at the end of the session must be the same that was charged in UC mode by the EV owner.
- **Exclusivity:** the EV cannot charge and discharge at the same time, so  $Y_{ch} + Y_{dch} \leq 1$  at each timestep.

Note that the V1G case is obtained by fixing  $Y_{dch}=0$  at each timestep. The problem is solved by making use of the Gurobi 10.0.0 solver for Python. The obtained SC (V1G and V2G) timeseries of charging/discharging power levels are used, together with the SoC and air temperature ones, for the battery degradation analysis.

#### D. Battery degradation model

The degradation model employed in this study is adapted from [19] and used to estimate the calendar and cycling ageing for the different charging strategies. The capacity fade due to calendar ageing ( $\Delta C_{cat}$ ), i.e. the % of lost battery capacity w.r.t. the nominal value, depends on the battery temperature, SoC and the time, as expressed by Eq. 2:

$$\Delta C_{cat}(\tau) = \frac{1}{2} \int_0^\tau \frac{p_j(t)}{\sqrt{t}} \cdot e^{-\frac{E_a}{R \cdot T_{batt}(t)}} \cdot dt \quad (2)$$

where:

- $p$  is the pre-exponential factor, which depends on SoC variation in time, and varies between  $300 \text{ h}^{-1/2}$  (SoC=0%) and  $1500 \text{ h}^{-1/2}$  (SoC=100%) [20].
- $E_a = 24500 \text{ J/mol}$  is the activation energy of the battery chemical reaction [20].
- $R = 8.314 \frac{\text{J}}{\text{mol} \cdot \text{K}}$  is the universal gas constant.
- $T_{batt}$  is the battery temperature in K, which is assumed to be 3-4°C higher than the ambient temperature [19].
- $t$  is the time in hours since the beginning of the recorded period.

Since the SoC value for the degradation model uses the real SoC, ranging from 10% to 90% of the nominal battery capacity, the reconstructed SoC profiles from the previous section are updated to never trespass those values.

The capacity fade caused cycling ageing ( $\Delta C_{cyc}$ ) depends on the battery temperature and current, as per Eq. 3.

$$\Delta C_{cyc}(\tau) = \vartheta \int_0^\tau B_1 \cdot e^{B_2(t)} \cdot |i(t)| \cdot dt \quad (3)$$

$$B_1(t) = a \cdot T_b(t)^2 + b \cdot T_b(t) + c$$

$$B_2(t) = (d \cdot T_b(t) + e) \cdot \rho_R(t)$$

where:

- $\vartheta = \frac{1.5}{C_{Ah} \cdot N_p}$  is a corrective factor to account for the battery cell size change from 1.5 Ah [19] to  $C_{Ah}$ . Since the electric parameters of the EVs are unknown, it is assumed that the energy density of the single cell, and its nominal voltage level are fixed at 200 Wh/g and 3.65 V, and that the other

electric parameters are the ones specified in the following table:

	$C_{kWh}$	$N_s$	$N_p$	$C_{Ah}$	$V_{batt}^{nom}$	$m_{batt}$
C1	14	55	2	45.0	200 V	88 kg
C2	21	55	4	32.5	200 V	130 kg
C3	95	110	4	74.6	400 V	591 kg

Where  $N_p$  and  $N_s$  are the number of cells in parallel and series,  $C_{Ah}$  is the cell capacity in Ah,  $C_{kWh}$  is the usable battery capacity in kWh,  $V_{batt}^{nom}$  is the nominal charging voltage of the battery, and  $m_{batt}$  is the estimated battery weight.

- $a=8.58 \cdot 10^{-6} A^{-1} h^{-1} K^{-2}$ ,  $b=-5.1 \cdot 10^{-3} A^{-1} h^{-1} K^{-1}$ ,  $c=0.7589 A^{-1} h^{-1}$ ,  $d=-6.7 \cdot 10^{-3} h K^{-1}$ ,  $e=2.344 \text{ h}$  are empirical coefficients [20].
- $i(t)$  is the current flowing through the battery, estimated by dividing the power signal by the nominal voltage.
- $\rho_R(t)$  is the C-rate of the EV battery under study, adjusted to consider a  $C_{Ah}$  battery capacity, instead of a 1.5 Ah one.

The SoH is thus obtained by combining calendar and cycling ageing (Eq. 4).

$$SoH = 100 - \Delta C_{calendar} - \Delta C_{cycling} \quad (4)$$

Assuming the EV charging profile to be constant along the 10 years of EV lifetime, the reconstructed SoC profile is updated after every year by considering the capacity fade. This is done by 1) equally modifying the  $SoC_{max}$  and  $SoC_{min}$  values to reflect the SoH variation, and 2) increasing the c-rate, since the usable battery capacity is smaller. In this way, both the calendar and cycling ageing values are updated to consider the yearly capacity fade.

## 4. Results and Discussion

The reconstructed SoC profiles for a year of charging are shown in Figure 3. The periods where the SoC slowly decreases represent the linearized driving sessions. As observed also from Table 1, C1 shows the highest charging frequency (once every 1.5 days) and duration (15.5 h), with the lowest charging energy per session (5.64 kWh). This is typical of an EV with a small battery (14 kWh usable), charging at low power (3.55 kW). C3 exhibits the opposite trend, performing the cycles with the deepest depth-of-discharge and median charged energy (56.85 kWh), and a much lower frequency (one session every 8 days).

The main outcomes from the EV scheduling optimisation are shown in Table 2. The results indicate there is minimal V2G activity, as evidenced by the negligible throughput increase compared to UC/V1G. This happens because the high difference between the charging/retail and discharging/day-ahead average electricity prices, e.g., 3.51 vs. 1.56 DKK/kWh (0.47 vs 0.21 €/kWh), makes it easier to just charge the car when it's cheaper (V1G), rather than pre-discharging it to make space for a longer session later

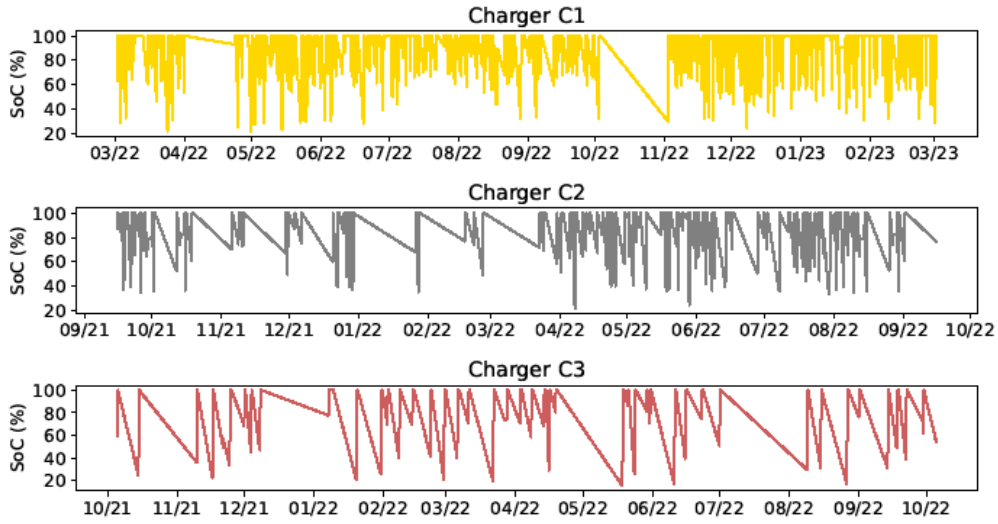


**Figure 3.** Reconstructed SoC Profiles for one year of usage in UC mode.

**Table 2.** Results of the EV scheduling process on a yearly basis.

	Connection time (h)	Throughput (MWh)		Full Cycles		Savings (DKK)		Savings (%)	
		UC/V1G	V2G	UC/V1G	V2G	V1G	V2G	V1G	V2G
<b>C1</b>	4148	2.38	2.52	67.9	89.8	1075.05	1141.76	20%	21.83%
<b>C2</b>	1144	1.79	1.90	34.1	45.1	575.31	667.57	13.54%	18.39%
<b>C3</b>	628	4.24	4.24	17.9	22.3	898.47	898.51	10.05%	10.05%

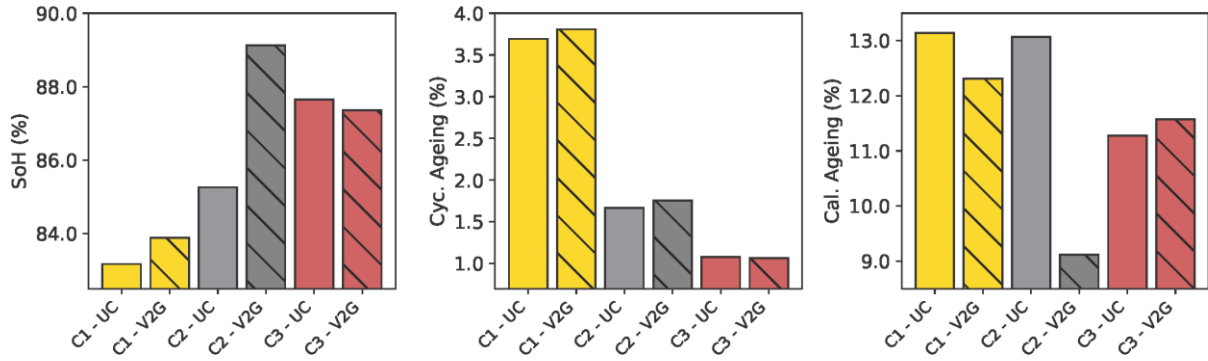


**Figure 4.** EV battery capacity degradation for the three chargers after 10 years of lifetime.

on (V2G). Considering other grid services or the inclusion of a vehicle-to-home policy could increase the V2G mode usage, but that is out of the scope of this article.

Thus, the majority of cost savings stem from V1G operations (10-20%), even if higher cost savings (10-22%, i.e. 668-1142 DKK or 89-153 € per year) are observed in V2G mode. The analysis reveals a positive correlation between connection time and savings, since the EV with the highest savings potential is C1, and a negative correlation between charging power and savings since the EV with the lowest CP phase charging power yields the highest savings potential.

The degradation results after 10 years for the UC and SC cases are presented in Figure 4. As shown by Eq. 2 and 3, calendar ageing exhibits an exponential trend with time, while cycling is linear with time, since the current profile is the same at each year. In all cases, the SoH after 10 years is above 83% and is mainly driven by calendar ageing. The

highest degradation is estimated for C1 at 83.2%, followed by C2 and C3 at 85.2% and 87.6%, respectively. This is because C1 has both high calendar (13.1%) and cycling ageing (3.69%) since its battery is small and almost always full (75% percent of the SoC values are over 79% usable SoC). The opposite can be observed for C3, where 75% of the values are over 55% usable SoC and the battery is larger, leading to a 1% cycling ageing, and 11.3% calendar one.

UC results are employed as the baseline to compare the trends observed for SC. Figure 4 compares V2G with UC in terms of total SoH, cycling, and calendar ageing. Note that only V2G is presented since its V2G throughput increase compared to V1G is almost null.

Figure 4 clearly shows that V2G generally decreases calendar ageing (due to the improvement from V1G), and only slightly increases cycling ageing. Significant SoH improvements are noticed in C2 only, a decrease of 3.86%,

associated to a calendar ageing reduction by 3.96%, and a cycling increase of 0.1%. The calendar decrease is due to 75% of the usable SoC values being higher than 51% (in SC), instead of 77% (in UC), a 26% difference. This difference reduces to 13% and 3% for C1 and C3, respectively, hence the similar calendar ageing values.

## 5. Conclusions

This study examined real residential EV charging data from Denmark and evaluated the effects of various smart charging strategies on battery degradation. To overcome the issue of the limited information included in current communication protocols, the study proposes a methodology to reconstruct SoC profiles based on charging power data only. SoC profiles for three distinct chargers were reconstructed and optimized, considering both uni- (V1G) and bi-directional (V2G) smart charging.

The analysis reveals that most of the cost-saving potential arises from V1G alone, primarily through shifting the charging sessions to low-cost periods, with savings up to 10-22% (575-1075 DKK or 77-144 € per year). The effect of V2G is minimal for the considered services, resulting in only marginal increases in cost savings (up to 92 DKK or 12 € in a year). Different types of services, such as such as frequency regulation, peak-shaving/valley-filling, or renewable energy sources following might yield more substantial cost savings and V2G activation, which will be explored in future works.

Calendar ageing emerges as the predominant degradation factor, with V1G allowing for a reduction of the degradation by maintaining SoC at lower levels, consequently reducing calendar ageing up to 4% over a decade. The slight rise in cycling ageing due to V2G is generally offset by the decrease in calendar ageing, confirming the results of prior research works on the topic and indicating that smart charging does not necessarily lead to an earlier EV battery retirement.

## Acknowledgement

This research has received funding from the European Union's Horizon 2020 research and innovation program under grant agreement No. 963580 (ALBATROSS Project) and Horizon Europe grant agreement 101056730 (FLOW Project).

The Authors would like to acknowledge the assistance of the RYC2021-033477-I grant (RyC2021 project), funded by NextGenerationEU/PRTR.

The Authors would also like to acknowledge Malthe Thingvad from Spirii, for providing the dataset on which this analysis is based. Lluc Canals Casals is a Serra Hunter Fellow.

## References

[1] O. Sadeghian, A. Oshnoei, B. Mohammadi-ivatloo, V. Vahidinasab, and A. Anvari-Moghaddam, "A comprehensive review on electric vehicles smart charging: Solutions, strategies,

technologies, and challenges," *Journal of Energy Storage*, vol. 54, p. 105241, Oct. 2022, doi: 10.1016/j.est.2022.105241.

[2] M. İnci, M. M. Savrun, and Ö. Çelik, "Integrating electric vehicles as virtual power plants: A comprehensive review on vehicle-to-grid (V2G) concepts, interface topologies, marketing and future prospects," *Journal of Energy Storage*, vol. 55, p. 105579, Nov. 2022, doi: 10.1016/j.est.2022.105579.

[3] J. D. K. Bishop, C. J. Axon, D. Bonilla, M. Tran, D. Banister, and M. D. McCulloch, "Evaluating the impact of V2G services on the degradation of batteries in PHEV and EV," *Applied Energy*, vol. 111, pp. 206–218, Nov. 2013, doi: 10.1016/j.apenergy.2013.04.094.

[4] T. Steffen, A. Fly, and W. Mitchell, "Optimal Electric Vehicle Charging Considering the Effects of a Financial Incentive on Battery Ageing," *Energies*, vol. 13, no. 18, p. 4742, Sep. 2020, doi: 10.3390/en13184742.

[5] M. Secchi, G. Barchi, D. Macii, and D. Petri, "Smart electric vehicles charging with centralised vehicle-to-grid capability for net-load variance minimisation under increasing EV and PV penetration levels," *Sustainable Energy, Grids and Networks*, vol. 35, p. 101120, Sep. 2023, doi: 10.1016/j.segan.2023.101120.

[6] D. Wang, J. Coignard, T. Zeng, C. Zhang, and S. Saxena, "Quantifying electric vehicle battery degradation from driving vs. vehicle-to-grid services," *Journal of Power Sources*, vol. 332, pp. 193–203, Nov. 2016, doi: 10.1016/j.jpowsour.2016.09.116.

[7] S. Bhoir, P. Caliendo, and C. Brivio, "Impact of V2G service provision on battery life," *Journal of Energy Storage*, vol. 44, p. 103178, Dec. 2021, doi: 10.1016/j.est.2021.103178.

[8] Y. Wei *et al.*, "A Comprehensive Study of Degradation Characteristics and Mechanisms of Commercial Li(NiMnCo)O<sub>2</sub> EV Batteries under Vehicle-To-Grid (V2G) Services," *Batteries*, vol. 8, no. 10, p. 188, Oct. 2022, doi: 10.3390/batteries8100188.

[9] K. Uddin, T. Jackson, W. D. Widanage, G. Chouchelamane, P. A. Jennings, and J. Marco, "On the possibility of extending the lifetime of lithium-ion batteries through optimal V2G facilitated by an integrated vehicle and smart-grid system," *Energy*, vol. 133, pp. 710–722, Aug. 2017, doi: 10.1016/j.energy.2017.04.116.

[10] P. Huang *et al.*, "Investigation of electric vehicle smart charging characteristics on the power regulation performance in solar powered building communities and battery degradation in Sweden," *Journal of Energy Storage*, vol. 56, p. 105907, Dec. 2022, doi: 10.1016/j.est.2022.105907.

[11] H. A. Gandhi and A. D. White, "City-Wide Modeling of Vehicle-to-Grid Economics to Understand Effects of Battery Performance," *ACS Sustainable Chem. Eng.*, vol. 9, no. 44, pp. 14975–14985, Nov. 2021, doi: 10.1021/acssuschemeng.1c05490.

[12] Mattia Secchi and Peter Bach Andersen, "Potential Barriers & Services of Vehicle-Grid Integration," Technical University of Denmark (DTU), 2023.

[13] Jelle Meersmans, "SCALE D1.5 - Analysis of hard- and software requirements," 2023. [Online]. Available: [https://scale-horizon.eu/?jet\\_download=5762](https://scale-horizon.eu/?jet_download=5762)

[14] Electric Nation, "Summary of the findings of the Electric Nation smart charging trial," Electric Nation, UK, 2019.

[15] Danish Meteorological Institute, "Meteorologens kommentar." Accessed: Jan. 24, 2024. [Online]. Available: <https://www.dmi.dk/meteorologens-kommentar>

[16] A. Thingvad, L. Calearo, P. B. Andersen, and M. Marinelli, "Empirical Capacity Measurements of Electric Vehicles Subject to Battery Degradation From V2G Services," *IEEE Trans. Veh. Technol.*, vol. 70, no. 8, pp. 7547–7557, Aug. 2021, doi: 10.1109/TVT.2021.3093161.

[17] International Electrotechnical Commission, "IEC 61851-1:2017 Electric vehicle conductive charging system - Part 1: General requirements." 2017.

[18] A. Thingvad, C. Ziras, and M. Marinelli, "Economic value of electric vehicle reserve provision in the Nordic countries under driving requirements and charger losses," *Journal of Energy Storage*, vol. 21, pp. 826–834, Feb. 2019, doi: 10.1016/j.est.2018.12.018.

[19] M. Marinelli, L. Calearo, and J. Engelhardt, "A Simplified Electric Vehicle Battery Degradation Model Validated with the Nissan LEAF e-plus 62-kWh," 2023.

[20] J. Wang *et al.*, "Degradation of lithium ion batteries employing graphite negatives and nickel-cobalt-manganese oxide + spinel manganese oxide positives: Part 1, aging mechanisms and life estimation," *Journal of Power Sources*, vol. 269, pp. 937–948, Dec. 2014, doi: 10.1016/j.jpowsour.2014.07.030.